View metadata, citation and similar papers at core.ac.uk

brought to you by CORE

provided by K-State Research Exchange

This is the author's final, peer-reviewed manuscript as accepted for publication. The publisher-formatted version may be available through the publisher's web site or your institution's library.

Comparison of the physical, chemical and electrical properties of ALD Al2O3 on c- and m-plane GaN

D. Wei, T. Hossain, N. Nepal, N. Y. Garces, J. K. Hite, H. M. Meyer III, C. R. Eddy, Jr., and J. H. Edgar

How to cite this manuscript

If you make reference to this version of the manuscript, use the following information:

Wei, D., Hossain, T., Nepal, N., Garces, N. Y., Hite, J. K., Meyer, H. M. III, Eddy, C. R. Jr., & Edgar, J. H. (2014). Comparison of the physical, chemical and electrical properties of ALD Al2O3 on c- and m-plane GaN. Retrieved from http://krex.ksu.edu

Published Version Information

Citation: Wei, D., Hossain, T., Nepal, N., Garces, N. Y., Hite, J. K., Meyer, H. M. III, Eddy, C. R. Jr., & Edgar, J. H. (2014). Comparison of the physical, chemical and electrical properties of ALD Al2O3 on c- and m-plane GaN. Physica Status Solidi C, 11(3-4), 898-901.

Copyright: © 2014 WILEY-VCH Verlag GmbH & Co. KGaA, Weinheim

Digital Object Identifier (DOI): doi:10.1002/pssc.201300677

Publisher's Link: http://onlinelibrary.wiley.com/doi/10.1002/pssc.201300677/abstract

This item was retrieved from the K-State Research Exchange (K-REx), the institutional repository of Kansas State University. K-REx is available at http://krex.ksu.edu

Review copy – not for distribution

(pss-logo will be inserted here by the publisher)

Comparison of the physical, chemical and electrical properties of ALD Al_2O_3 on *c*- and *m*-plane GaN

D. Wei[1], T. Hossain[1], N. Nepal[2], N.Y. Garces[2], J.K. Hite[2], H.M. Meyer III[3], C.R. Eddy, Jr.[2] and J.H. Edgar[*,1]

[1] Department of Chemical Engineering, Kansas State University, Manhattan, KS, 66506, USA
[2] Electronics Science and Technology Division, Naval Research Laboratory, 4555 Overlook Ave, S.W. Washington, DC 20375, USA
[3] Materials Science and Technology Division, Oak Ridge National Laboratory, Oak Ridge, TN, 37831-6064, USA

Received ZZZ, revised ZZZ, accepted ZZZ
Published online ZZZ (Dates will be provided by the publisher.)

Keywords ALD, dielectric, *m*-plane, GaN

This study compares the physical, chemical and electrical properties of Al_2O_3 thin films deposited on gallium polar *c*- and nonpolar *m*-plane GaN substrates by atomic layer deposition (ALD). Correlations were sought between the film's structure, composition, and electrical properties. The thickness of the Al_2O_3 films was 19.2 nm as determined from a Si witness sample by spectroscopic ellipsometry. The gate dielectric was slightly aluminum-rich (Al:O=1:1.3) as measured from x-ray photoelectron spectroscopy (XPS) depth profile, and the oxide-semiconductor interface carbon concentration was lower on *c*-plane GaN. The oxide's surface morphology was similar on both substrates, but was smoothest on *c*-plane GaN as determined by atomic force microscopy (AFM). Circular capacitors (50-300 µm diameter) with Ni/Au (20/100 nm) metal contacts on top of the oxide were created by standard photolithography and e-beam evaporation methods to form metal-oxide-semiconductor capacitors (MOSCAPs). The alumina deposited on *c*-plane GaN showed less hysteresis (0.15V) than on *m*-plane GaN (0.24V) in capacitance-voltage (CV) characteristics, consistent with its better quality of this dielectric as evidenced by negligible carbon contamination and smooth oxide surface. These results demonstrate the promising potential of ALD Al_2O_3 on *c*-plane GaN, but further optimization of ALD is required to realize the best properties of Al_2O_3 on *m*-plane GaN.

Copyright line will be provided by the publisher

1 Introduction GaN is employed for power electronics because of its ability to operate at high temperatures, high frequencies, and high power. For instance, in AlGaN high electron mobility transistors (HEMTs) high frequencies are achieved by the two dimensional electron gas (2DEG) that spontaneously forms at the AlGaN/GaN interface in the *c*-plane. These devices have a negative threshold voltage (normally-on transistor). For power applications, normally-off transistors are preferred for fail-safe operations and to minimize stand-by energy consumption [1]. As such, *m*-plane AlGaN/GaN heterostructures are promising for E-mode (normally-off) transistors due to the lack of a high-density, polarization induced 2DEG [2], but the performance of this *m*-plane heterostructure remains largely unexplored.

By incorporating an insulated gate, the metal insulator semiconductor high electron mobility transistor (MISHEMT) has the advantages of a lower leakage current, and larger voltage swings are possible compared to the HEMT. Many studies have been conducted on the gate oxide on *c*-plane GaN [3–5]; however research of high k oxide on *m*-plane GaN is also needed to optimize the device. This is addressed in this paper. The high-k gate dielectric Al_2O_3 was deposited by atomic layer deposition (ALD) on both *c*- and *m*-plane GaN. The physical, chemical and electrical properties of the oxide were compared and correlated to the performance of the devices.

2 Experiments The Ga-polar *c*-plane (0001) 2µm thick *n*-type ($1x10^{18}$ cm^{-3}) GaN film was deposited by metal oxide chemical vapour deposition (MOCVD) on *c*-plane sapphire. The non-polar GaN ($10\bar{1}0$) layer was prepared by GaN MOCVD on a pure *m*-plane GaN substrate with a 0.08 offcut angle towards the *c*-plane. The epitaxial layer was employed to ensure the surface was free of defects that might be present from substrate preparation such as chemi-

Copyright line will be provided by the publisher

cal mechanical polishing. Both the Ga-polar and non-polar GaN surface were cleaned with a piranha solution (H_2O_2:H_2SO_4 1 : 5) at 80ºC for 10 min before ALD. Al_2O_3 was deposited using 200 ALD cycles at 280ºC on the two different substrates. The thickness of the film was estimated to be 19.2 nm by using a variable angle spectroscopic ellipsometer (VASE) on Si witness samples. The Al_2O_3 film morphology was measured by atomic force microscope (AFM, Digital Instrument MultiMode SPM from Veeco Instruments Inc) operating in tapping mode. The composition of the ALD oxides was determined as a function of depth by x-ray photoelectron spectroscopy (XPS) with argon ion sputtering using a K-Alpha XPS from Thermo Scientific. For depth profiling of the composition, the ALD oxides were sputtered using 3 KV Ar-ions and set to a known sputtering rate for SiO_2, which is 6nm/min, as calibrated on a SiO_2 standard. 50-µm-diameter circular capacitors with Ni/Au (20/100 nm) metal contacts on top of the oxide were created by standard photolithography and e-beam evaporation methods (Fig. 1).

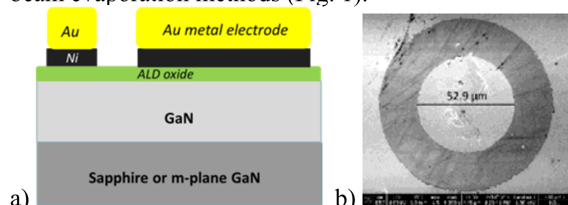

Figure 1 a) Schematic structure of the side view of the MOSCAP. b) Scanning electron microscopy (SEM) top view of the MOSCAP with the diameter of 52.9 µm.

The electrical properties of the gate dielectric were measured on the MOSCAPs by capacitance-voltage (C-V) measurements at room temperature. The area of the larger contact is four orders of magnitude higher than the device under test (DUT, Left MOSCAP in Fig. 1a), thus its contribution to the overall capacitance is negligible. Hysteresis sweeps were conducted with a DC bias of 4V to -6V at 1MHz with a sweep rate of 0.02V/s. Current-voltage (I-V) measurement was conducted with the large area contact as the low potential. Because of the big difference in areas, the total resistance of large area is not significant comparing to the resistance of DUT.

3 Results and discussion The surface morphology of the ALD Al_2O_3 films are shown in Fig. 2. Based on a relative small area (1x1 µm^2) AFM scan, both Al_2O_3 films are uniform and smooth with similar morphologies on *c*- and *m*-plane GaN substrate. This indicating the piranha pretreatment yielded a favourable condition for the initiation of ALD.

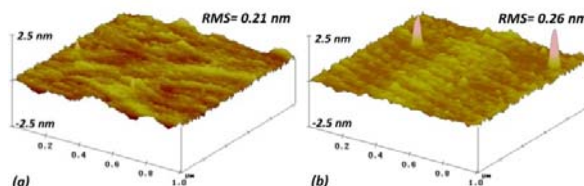

Figure 2 Three-dimensional AFM images of Al_2O_3 on (a) *c*-plane and (b) *m*-plane GaN. The Z height is 5nm and scan area is 1x1 square micron for both images.

However, under the larger area view by optical microscopy the surface of the *m*-plane GaN was covered in steps from the epitaxial layer by MOCVD (Fig. 3.). This is probably due to a small offcut angle of 0.08^0 toward *c*-plane GaN. A smooth surface was reported for substrate with 2^0 offcut angle towards *c*-plane [6,7].

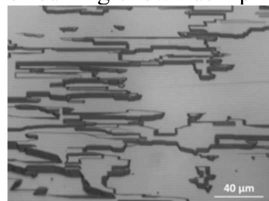

Figure 3 Optical microscopic image of the *m*-plane GaN surface. The morphology is a consequence of the epitaxial growth.

The depth profiles of the Al_2O_3 are shown in Fig. 4. Similar etching time of the films was observed on both *c*- and *m*-plane GaN; The gate oxides were slightly aluminum-rich with stoichiometry of Al:O=1:1.3 (~14% oxygen deficient) for the films on both *c*- and *m*-plane GaN. These proved ALD of Al_2O_3 yielded similar film composition regardless of the substrate used. The step structure on the *m*-plane GaN blocked part of the ion gun sputtering area, which led a residue signal of ~5% Al, O and 2% C. Less than 1% of fluorine was detected on the surface but disappeared after first round sputtering indicating fluorine was surface contamination.

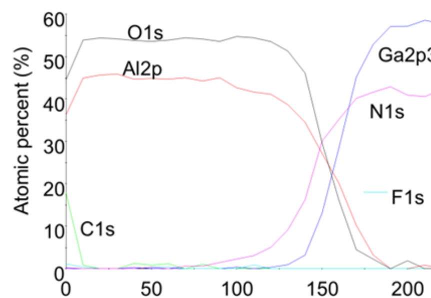

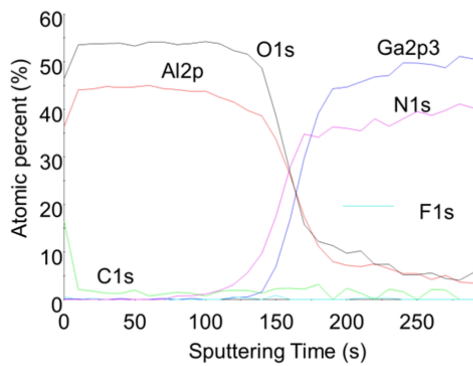

Figure 4 XPS depth profile of Al_2O_3 on a) *c*- and b) *m*-plane GaN.

Figure 5 showed hysteresis sweeps from the room temperature C-V measurement on the MOSCAPs on a) *c*- and b) *m*-plane GaN. The hysteresis was smaller on *c*-plane GaN. Also its change between the accumulation and depletion regions was sharper, indicating a lower trap density [8]. The step feature (Fig.3) on the surface of the *m*-plane GaN led to overall rougher surface, which could be detrimental for the electrical performance of MOSCAP [9], as it could form interface traps and cause a stretched-out depletion region in Fig. 5b.

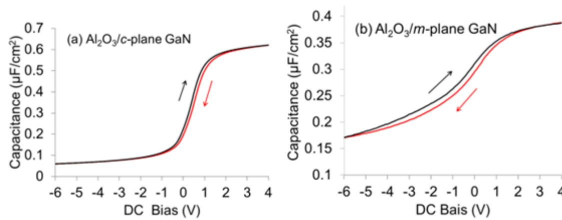

Figure 5 C-V measurements of the MOSCAPs on (a) *c*- and (b) *m*-plane GaN at 20 ^{0}C.

The total trapped charge was estimated by multiplying the hysteresis at the flat band voltage (V_{FB}) and the oxide capacitance (C_{ox}); V_{FB} was determined based on the flat band capacitance (C_{FB}) of the C-V measurement by [10]:

$$C_{FB} = \frac{C_{ox}\varepsilon_0\varepsilon_s A/\lambda}{\varepsilon_0\varepsilon_s A/\lambda + C_{ox}}$$

where C_{ox} is the determined from the accumulation region of the C-V curve; ε_0 is the permittivity of vacuum; ε_s is the dielectric constant of GaN (ε_s=9); A is the area of DUT; λ is the Debye length, and

$$\lambda = \sqrt{\varepsilon_s kT/q^2 N_D}$$

where k is the Boltzmann constant, and N_D is the doping concentration. The calculated results were listed in Table 1. The Al_2O_3 on the *c*-plane GaN had a slightly lower trapped density: $5.68\text{x}10^{11}$ cm^{-2} compared to $5.83\text{x}10^{11}cm^{-2}$ for Al_2O_3 on the *m*-plane. The larger hysteresis showing on the C-V of *m*-plane GaN yielding similar trapped density is because the capacitance of the MOSCAP fabricated on *m*-plane GaN is lower than *c*-plane GaN under the same DC bias in the accumulation region of the CV curve. Also, the capacitance did not reach saturation within the sweep range, possibly because the Fermi level was pinned for the *m*-plane GaN due to the high interface trap density [11,12], which also corresponded to its stretching out C-V curve [13]. High interface traps were also observed by Hung *et al.* [14], and could be suppressed by a 500°C post metal annealing (PMA) which was not performed in this study.

Table 1 Calculated oxide capacitance, flat band capacitance, hysteresis and total trapped charge density of Al_2O_3 on *c*- and *m*-plane GaN.

	C_{ox} (μF/cm^2)	C_{FB} (μF/cm^2)	hysteresis at V_{FB} (V)	Total trapped charge ($\text{x}10^{11}cm^{-2}$)
c-plane GaN	0.62	0.49	0.15	5.68
m-plane GaN	0.39	0.33	0.24	5.83

The leakage current were compared at +3V, equivalent to an electric field of 1.5MV/cm (Fig. 6). Although, *m*-plane GaN showed a slightly lower leakage current of $0.3\text{x}10^{-12}$A than *c*-plane GaN of $7.6\text{x}10^{-12}$A, the ALD Al_2O_3 layers were highly insulating on both orientations.

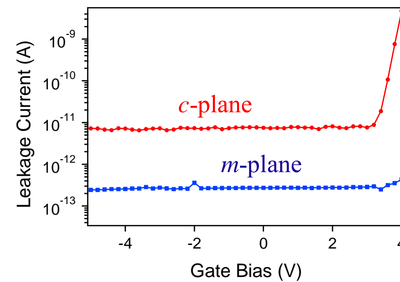

Figure 6 I-V measurement of the MOSCAPs on *c*- and *m*-plane GaN.

4 Conclusions

The oxide film shared similar thickness, surface morphology and stoichiometry regardless of substrate indicating the consistency of ALD procedure. The lower hysteresis and more abrupt change between accumulation and depletion region demonstrated better electrical properties of the ALD film on the *c*-plane than on the *m*-plane GaN. This could be improved by making smooth surface *m*-GaN with less crystal growth defects, and the performance of Al_2O_3 on low roughness *m*-GaN need to be further optimized.

Acknowledgements This study was supported by the Office of Naval Research (ONR) with grant number N00014-09-1-1160. The XPS work was sponsored by the Assistant Secretary for Energy Efficiency and Renewable Energy, Office of FreedomCAR and Vehicle Technologies, as part of the High Temperature Materials Laboratory User Program, Oak Ridge National

Copyright line will be provided by the publisher

Laboratory, managed by UT-Battelle, LLC, for the U.S. Department of Energy under contract number DE-AC05-00OR22725.

References

[1] R.D. Long and P.C. McIntyre, Materials (Basel). **5**, 1297 (2012).
[2] T. Fujiwara, R. Yeluri, D. Denninghoff, J. Lu, S. Keller, J.S. Speck, S.P. DenBaars, and U.K. Mishra, Appl. Phys. Express **4**, 096501 (2011).
[3] X. Sun, O.I. Saadat, K.S. Chang-Liao, T. Palacios, S. Cui, and T.P. Ma, Appl. Phys. Lett. **102**, 103504 (2013).
[4] M. Esposto, S. Krishnamoorthy, D.N. Nath, S. Bajaj, T.-H. Hung, and S. Rajan, Appl. Phys. Lett. **99**, 133503 (2011).
[5] M. Kanamura, T. Ohki, T. Kikkawa, K. Imanishi, T. Imada, A. Yamada, and N. Hara, IEEE ELECTRON DEVICE Lett. **31**, 189 (2010).
[6] M. Rudziński, R. Kudrawiec, L. Janicki, J. Serafinczuk, R. Kucharski, M. Zając, J. Misiewicz, R. Doradziński, R. Dwiliński, and W. Strupiński, J. Cryst. Growth **328**, 5 (2011).
[7] H. Masui, H. Yamada, K. Iso, S. Nakamura, and S.P. DenBaars, Appl. Phys. Lett. **92**, 091105 (2008).
[8] J.D. Plummer, M. Deal, and P.D. Griffin, *Silicon VLSI Technology: Fundamentals, Practice, and Modeling* (Prentice Hall, 2000), p. 817.
[9] N. Nepal, N.Y. Garces, D.J. Meyer, J.K. Hite, M. a. Mastro, and J.. C.R. Eddy, Appl. Phys. Express **4**, 055802 (2011).
[10] E.H. Nicollian and J.R. Brews, *MOS Physics and Technology.pdf* (1982), pp. 487–488.
[11] Y. Hwang, R. Engel-Herbert, N.G. Rudawski, and S. Stemmer, J. Appl. Phys. **108**, 034111 (2010).
[12] K. Martens, W. Wang, K. De Keersmaecker, G. Borghs, G. Groeseneken, and H. Maes, Microelectron. Eng. **84**, 2146 (2007).
[13] D. Shahrjerdi, M.M. Oye, A.L. Holmes, and S.K. Banerjee, Appl. Phys. Lett. **89**, 043501 (2006).
[14] T.-H. Hung, S. Krishnamoorthy, M. Esposto, D. Neelim Nath, P. Sung Park, and S. Rajan, Appl. Phys. Lett. **102**, 072105 (2013).

Copyright line will be provided by the publisher